DOI: 10.1021/ic1007582

Inorganic Chemistry
Article

Intramolecular NH···Pt Interactions of Platinum(II) Diimine Complexes with Phenyl Ligands

Sayandev Chatterjee,[†] Jeanette A. Krause,[†] Allen G. Oliver,[‡] and William B. Connick*[,†]

[†]*Department of Chemistry, University of Cincinnati, P.O. Box 210172, Cincinnati, Ohio 45221-0172, United States, and* [‡]*Department of Chemistry and Biochemistry, University of Notre Dame, Notre Dame, Indiana 46556, United States*

Received April 20, 2010

$Pt(pipNC)_2(phen)$ [$pipNC^-$ = 1-(piperidylmethyl)phenyl anion; phen = 1,10-phenanthroline] was prepared by the reaction of *cis*-$Pt(pipNC)_2$ with phen. Crystallographic and ^1H NMR data establish that the phen ligand is bidentate, whereas each piperidyl ligand is monodentate and bonded to the platinum at the ortho position of the phenyl group. Acidic conditions allowed for isolation of the salts of diprotonated $Pt(pipNHC)_2(diimine)^{2+}$ adducts (diimine = phen, 2,2′-bipyridine, or 5,5′-ditrifluoromethyl-2,2′-bipyridine). Crystallographic and spectroscopic data for the diprotonated complexes are consistent with H···Pt interactions (2.32−2.51 Å) involving the piperidinium groups, suggesting that the metal center behaves as a Brønsted base. Metal-to-ligand (diimine) charge-transfer states of $Pt(pipNHC)_2(phen)^{2+}$ in solution are strongly destabilized (>2500 cm^{-1}) relative to $Pt(pipNC)_2(phen)$, in keeping with the notion that NH···Pt interactions effectively reduce the electron density at the metal center. Though N···Pt interactions in $Pt(pipNC)_2(phen)$ appear to be weaker than those found for outer-sphere two-electron reagents, such as $Pt(pip_2NCN)(tpy)^+$ [pip_2NCN^- = 1,3-bis(piperidylmethylphenyl anion; tpy = 2,2′:6′,2′-terpyridine], each of the $Pt(pipNC)_2(diimine)$ complexes undergoes diimine ligand dissociation to give back *cis*-$Pt(pipNC)_2$ and free diimine ligand. Electrochemical measurements on the deprotonated complexes suggest that the piperidyl groups help to stabilize higher oxidation states of the metal center, whereas protonation of the piperidyl groups has a destabilizing influence.

Introduction

The availability of dangling nucleophilic groups near the axial sites of square-planar platinum(II) complexes can have a profound influence on the reactivity and electronic structure.[1−3] For example, $Pt(tpy)(pip_2NCN)^+$ (Scheme 1) undergoes nearly reversible cooperative two-electron transfer at 0.4 V vs Ag/AgCl (ΔE_p = 43 mV, 0.01 V/s), whereas the complex lacking piperidyl groups [i.e., $Pt(tpy)(2,6\text{-}dmph)^+$; $2,6\text{-}dmph^-$ = 2,6-dimethylphenyl anion] is not oxidized at <1.3 V.[4,5] The observed behavior is consistent with inversion of the one-electron redox potentials [i.e., $E_1°'(d^6/d^7) < E_2°'(d^7/d^8)$] and coordination of the piperidyl groups to the d^6-electron metal center to give a six-coordinate complex. The remarkable reversibility of this reaction, as well as spectroscopic and crystallographic data, have led to the suggestion

Scheme 1. $Pt(tpy)(pip_2NCN)^+$ and $Pt(pipNC)_2(phen)$

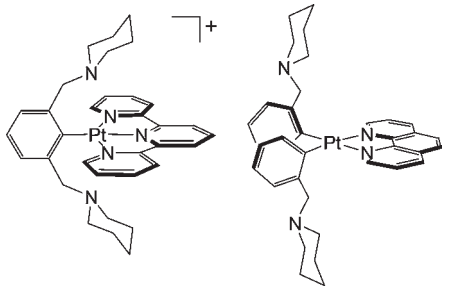

$Pt(pip_2NCN)(tpy)^+$ $Pt(pipNC)_2(phen)$

*To whom correspondence should be addressed. E-mail: bill.connick@uc.edu. Fax: (+1) 513-556-9239.

(1) For example, see:(a) Dixon, K. R. *Inorg. Chem.* **1977**, *16*, 2618–2624. (b) Sarneski, J. E.; McPhail, A. T.; Onan, K. D.; Erickson, L. E.; Reilley, C. N. *J. Am. Chem. Soc.* **1977**, *99*, 7376–7378. (c) Wieghardt, K.; Koppen, M.; Swiridoff, W.; Weiss, J. *J. Chem. Soc., Dalton Trans.* **1983**, 1869–1872. (d) Nikol, H.; Bürgi, H.-B.; Hardcastle, K. I.; Gray, H. B. *Inorg. Chem.* **1995**, *34*, 6319–6322. (e) Grant, G. J.; Spangler, N. J.; Setzer, W. N.; Van Derveer, D. G.; Mehne, L. F. *Inorg. Chim. Acta* **1996**, *246*, 31–40. (f) Davies, M. S.; Hambley, T. W. *Inorg. Chem.* **1998**, *37*, 5408–5409. (g) Wong, K.-H.; Chan, M. C.-W.; Che, C.-M. *Chem.—Eur. J.* **1999**, *5*, 2845–2849. (h) Prokopchuk, E. M.; Jenkins, H. A.; Puddephatt, R. J. *Organometallics* **1999**, *18*, 2861–2866. (i) Yip, J. H. K.; Suwarno; Vittal, J. J. *Inorg. Chem.* **2000**, *39*, 3537–3543. (j) Shi, J.-C.; Chao, H.-Y.; Fu, W.-F.; Peng, S.-M.; Che, C.-M. *Dalton Trans.* **2000**, 3128–3132. (k) Green, T. W.; Lieberman, R.; Mitchell, N.; Krause, J. A.; Connick, W. B. *Inorg. Chem.* **2005**, *44*, 1955–1965.

(2) Blake, A. J.; Gould, R. O.; Holder, A. J.; Hyde, T. I.; Lavery, A. J.; Odulate, M. O.; Schroder, M. *J. Chem. Soc., Chem. Commun.* **1987**, 118–120.

(3) Vedernikov, A. N.; Pink, M.; Caulton, K. G. *Inorg. Chem.* **2004**, *43*, 3642–3646.

(4) Jude, H.; Carroll, G. T.; Connick, W. B. *Chemtracts* **2003**, *16*, 13–22.

(5) Jude, H.; Krause Bauer, J. A.; Connick, W. B. *J. Am. Chem. Soc.* **2003**, *125*, 3446–3447.

Published on Web 10/08/2010

that the dangling piperidyl groups interact with the Pt^{II} center prior to or during anodic electron transfer, effectively preorganizing the molecule for electron transfer.[4,5] Interestingly, although there are a number of platinum complexes with ligand architectures capable of stabilizing the d^8-electron square-planar and d^6-electron octahedral coordination geometries, those systems are typically characterized by chemically irreversible redox reactions or selective stabilization of the d^7-electron adduct, consistent with $E_2^{\circ\prime}(d^7/d^8) < E_1^{\circ\prime}(d^6/d^7)$.[6]

To better understand the properties of $Pt(tpy)(pip_2NCN)^+$, we have prepared structural and electronic analogues. Here we report the synthesis and properties of $Pt(pipNC)_2$(diimine) complexes, such as $Pt(pipNC)_2$(phen) (Scheme 1), and their protonated adducts, $Pt(pipNHC)_2(diimine)^{2+}$. Structural, spectroscopic, and electrochemical results suggest that the metal in $Pt(pipNC)_2$(diimine) complexes has significant Brønsted base character. In the case of the protonated adducts, NH···Pt interactions have a profound influence on the electronic structures.

Experimental Section

General Considerations. K_2PtCl_4 was obtained from Pressure Chemical Co. All other reagents were purchased from Acros. Tetrahydrofuran (THF) was distilled from Na(s) and benzophenone. $Pt(COD)Cl_2$,[7] Pt(phen)(Ph)$_2$ (Ph = phenyl),[8] 2-(bromomethyl)bromobenzene, 2-($CH_2(C_5H_{10}N)$)C_6H_3Br(pipNCBr),[9] and 5,5′-ditrifluoromethyl-2,2′-bipyridine (dtfmbpy)[10] were prepared according to literature procedures. Syntheses involving amines were carried out in an inert argon atmosphere using standard Schlenk techniques. Argon was predried using activated sieves, and trace impurities of oxygen were removed with activated R3-11 catalyst from Schweizerhall.

^{1}H NMR spectra were recorded at room temperature using a Bruker AC 400 MHz instrument. Deuterated solvents $CDCl_3$ [0.03% tetramethylsilane (TMS) (v/v)], CD_3CN, and CD_2Cl_2 were purchased from Cambridge Isotope Laboratories. UV−visible absorption spectra were recorded using a HP8453 UV−visible spectrophotometer. Mass spectra were obtained by electrospray ionization of acetonitrile solutions using a Micromass Q-TOF-2 instrument.

Cyclic voltammetry measurements were carried out using a standard three-electrode cell and a 100 B/W electrochemical workstation from Bioanalytical Systems. Scans were recorded of solutions containing 0.1 M $TBAPF_6$. All scans were recorded using a platinum wire auxiliary electrode and gold or platinum working electrodes. The use of glassy carbon working electrodes resulted in electrode passivation and, consequently, was avoided. Between measurements, the working electrode was polished with 0.05 μm alumina, rinsed with distilled water, and wiped dry using a Kimwipe. All reported potentials are referenced vs Ag/AgCl (3.0 M NaCl). Peak currents (i_p) were estimated with respect to the extrapolated baseline current, as described by Kissinger and Heineman.[11]

***cis*-Pt(pipNC)$_2$.** All glassware and reagents were rigorously dried prior to use. Under an argon gas atmosphere, *N*-butyllithium (3.42 mL of a 1.6 M solution in hexanes, 5.5 mmol) was added to a stirred solution of pipNCBr (1.52 g, 6.0 mmol) in 20 mL of THF at −70 °C. After 30 min, the solution of lithiated ligand was cannula-transferred to a mixture of $Pt(COD)Cl_2$ (0.93 g, 2.5 mmol) in 75 mL of THF at −70 °C. The mixture was stirred for 1 h at −70 °C, warmed to room temperature, and then stirred for an additional 12 h. The filtrate was rotary-evaporated to dryness. Water (50 mL) was added to the solid, and the product was extracted with CH_2Cl_2 (3 × 50 mL). The organic layers were dried over anhydrous $MgSO_4$ and rotary-evaporated to dryness. After the addition of hexanes to the residue, the mixture was sonicated, and the white solid was collected. Yield: 0.82 g, 61%. Anal. Calcd for $C_{24}H_{32}N_2Pt$: C, 53.03 H, 5.93; N, 5.12. Found: C, 53.17; H, 5.85; N, 5.12. ^{1}H NMR ($CDCl_3$, δ): 1.35−1.6 (4H, m, CH_2), 1.85−2.0 (8H, m, CH_2), 3.21 (4H, m, CH_2), 3.36 (4H, m, CH_2), 4.23 (4H, s with Pt satellites, J_{H-Pt} = 21 Hz, benzylic CH_2), 6.9−7.0 (5H, m, CH), 7.31 (2H, t, CH), 7.41 (1H, d with Pt satellites, J_{H-Pt} = 50 Hz, CH).

Pt(pipNC)$_2$(phen). A mixture of *cis*-Pt(pipNC)$_2$ (54 mg, 0.1 mmol) and 1,10-phenanthroline (18 mg, 0.1 mmol) in dichloromethane (30 mL) was refluxed for 3 h. The resulting yellow-orange solution was rotary-evaporated to dryness to give an orange-yellow solid. The product was contaminated with starting materials and is unstable in solution (see the text). Using a chloroform or dichloroethane solvent produces similar results. The complex also is readily prepared in situ by deprotonation of $Pt(pipNHC)_2(phen)^{2+}$ with 2 equiv of TBAOH. ^{1}H NMR (CD_2Cl_2, δ): 0.89−3.59 (overlapping with TBAOH resonances), 3.93 (1.6H, dd,), 4.09 (2.4H, dd), 6.87 (2H, dd, J_{H-H} = 11.2 and 5.6 Hz), 6.92 (2H, dd, J_{H-H} = 11.2 and 7.2 Hz), 7.32 (2H, d, J_{H-H} = 8 Hz), 7.61 (2H, dd, J_{H-H} = 6.4 and 3.2 Hz), 7.66 (2H, d, J_{H-H} = 4 Hz), 7.99 (2H, s), 8.52 (2H, d, J_{H-H} = 8 Hz), 8.60 (2H, d, J_{H-H} = 8 Hz).

[Pt(pipNHC)$_2$(phen)](PF$_6$)$_2$. Trifluoroacetic acid (14.7 μL, 0.2 mmol) was added to a suspension of *cis*-Pt(pipNC)$_2$ (54 mg, 0.1 mmol) in acetonitrile (30 mL). The mixture was stirred and sonicated, and an equimolar amount of 1,10-phenanthroline (18 mg, 0.1 mmol) was added to the resulting solution. The mixture was refluxed for 3 h, and the yellow solution was allowed to cool to room temperature. NH_4PF_6 (41 mg, 0.25 mmol) was added, and the solution was rotary-evaporated to dryness. The product was dissolved in a minimum amount of acetonitrile, and diethyl ether was added to induce precipitation. Yield: 0.072 g, 71%. Anal. Calcd for $C_{36}H_{42}F_{12}N_4P_2Pt$: C, 42.57; H, 4.17; N, 5.52. Found: C, 42.35; H, 4.17; N, 5.51. ^{1}H NMR (CD_3CN, δ): 0.87 (2H, m), 1.276 (2H, m), 1.46 (6H, m), 1.74 (2H, m), 2.50 (2H, dd, α-H, J_{H-H} = 12.0 and 8.6 Hz), 2.91 (2H, dd, α-H, J_{H-H} = 16.0 and 8.0 Hz), 3.10 (2H, d, α-H, J_{H-H} = 6.4 Hz), 3.39 (2H, d, α-H, J_{H-H} = 10.0 Hz), 3.76 (2H, dd, benzylic CH_2, J_{H-H} = 12.8 and 2.4 Hz), 3.88 (2H, dd, benzylic CH_2, J_{H-H} = 12.8 and 2.4 Hz), 7.11 (2H, d, J_{H-H} = 8.0 Hz), 7.20 (2H, dd, J_{H-H} = 9.6 and 7.2 Hz), 7.36 (2H, dd, J_{H-H} = 9.6 and 5.6 Hz), 7.93 (2H, dd, J_{H-H} = 15.2 and 7.6 Hz), 7.95 (2H, dd, J_{H-H} = 16.8 and 8.4), 8.02 (2H, s, N−H), 8.25 (2H, s), 8.57 (2H, d, J_{H-H} = 4.4 Hz), 8.86 (2H, d, J_{H-H} = 8.0 Hz). ^{1}H NMR (CD_2Cl_2, δ): 0.99 (2H, m), 1.43−1.53 (8H, m), 1.87 (2H, m), 2.51 (2H, d, α-H, J_{H-H} = 7.6 Hz), 2.98 (2H, d, α-H, J_{H-H} = 8.4 Hz), 3.16 (2H, d, α-H, J_{H-H} = 10.8 Hz), 3.47 (2H, d, α-H, J_{H-H} = 10.8 Hz), 3.71 (2H, dd, benzylic CH_2, J_{H-H} = 13.2 and 2.4 Hz), 3.94 (2H, dd, benzylic CH_2, J_{H-H} = 7.2 and 2.4 Hz), 7.20 (2H, d, J_{H-H} = 13.2 Hz), 7.29 (2H, dd, J_{H-H} = 6.8 and 6.4 Hz), 7.43 (2H, dd, J_{H-H} = 8.8

(6) For example, see:(a) Boucher, H. A.; Lawrance, G. A.; Lay, P. A.; Sargeson, A. M.; Bond, A. M.; Sangster, D. F.; Sullivan, J. C. *J. Am. Chem. Soc.* **1983**, *105*, 4652–4661. (b) Blake, A. J.; Gould, R. O.; Holder, A. J.; Hyde, T. I.; Lavery, A. J.; Odulate, M. O.; Scrhöder, M. *J. Chem. Soc., Dalton Trans.* **1987**, 118–120. (c) McAuley, A.; Whitcombe, T. W. *Inorg. Chem.* **1988**, *27*, 3090–3099. (d) Blake, A. J.; Holder, A. J.; Roberts, Y. V.; Schroder, M. *J. Chem. Soc., Chem. Commun.* **1993**, 260–262. (e) Grant, G. J.; Spangler, N. J.; Setzer, W. N.; Van Derveer, D. G.; Mehne, L. F. *Inorg. Chim. Acta* **1996**, *246*, 31–40. (f) Brown, K. N.; Hockless, D. C. R.; Sargeson, A. M. *J. Chem. Soc., Dalton Trans.* **1999**, 2171–2176. (g) Matsumoto, M.; Funahashi, S.; Takagi, H. D. *Z. Naturforsch.* **1999**, *54B*, 1138–1146. (h) Matsumoto, M.; Itoh, M.; Funahashi, S.; Takagi, H. D. *Can. J. Chem.* **1999**, *77*, 1638–1647. (i) Haines, R. I.; Hutchings, D. R.; McCormack, T. M. *J. Inorg. Biochem.* **2001**, *85*, 1–7. (j) Brown, K. N.; Geue, R. J.; Hambley, T. W.; Hockless, D. C. R.; Rae, A. D.; Sargeson, A. M. *Org. Biomol. Chem.* **2003**, *1*, 1598–1608.

(7) McDermott, J. X.; White, J. F.; Whitesides, G. M. *J. Am. Chem. Soc.* **1976**, *98*, 6521–6528.

(8) Klein, A.; McInnes, E. J. L.; Kaim, W. *J. Chem. Soc., Dalton Trans.* **2002**, 2371–2378.

(9) Mehta, N. B.; Strelitz, J. Z. *J. Org. Chem.* **1962**, *27*, 4412–4418.

(10) Chan, K. S.; Tse, A. K.-S. *Synth. Commun.* **1993**, *23*, 1929–1934.

(11) Kissinger, P. T.; Heineman, W. R. *J. Chem. Educ.* **1983**, *60*, 702–706.

and 8.0 Hz), 7.73 (2H, s, N−H), 7.92 (2H, dd, J_{H-H} = 8.4 and 5.2 Hz), 7.97 (2H, d, J_{Pt-H} = 60.8 Hz, J_{H-H} = 7.6 Hz), 8.19 (2H, s), 8.49 (2H, d, J_{H-H} = 4.8 Hz), 8.77 (2H, d, J_{H-H} = 8.0 Hz). MS-ESI (*m*/*z*): 870.78, $[Pt(pipNHC)_2(phen)](PF_6)^+$; 724.82, $[Pt(pipNHC)(pipNC)(phen)]^+$.

[Pt(pipNHC)$_2$(bpy)](PF$_6$)$_2$. Trifluoroacetic acid (14.7 μL, 0.2 mmol) was added to a suspension of *cis*-Pt(pipNC)$_2$ (54 mg, 0.1 mmol) in acetonitrile (30 mL). The mixture was stirred and sonicated, and an equimolar amount of 2,2′-bipyridine (15.6 mg, 0.1 mmol) was added to the resulting solution. The mixture was refluxed for 3 h, and the yellow solution was allowed to cool to room temperature. NH_4PF_6 (41 mg, 0.25 mmol) was added, and the resultant solution was rotary-evaporated to dryness. The product was dissolved in a minimum amount of acetonitrile, and diethyl ether was added to induce precipitation. Yield: 0.062 g, 63%. Anal. Calcd for $C_{34}H_{42}F_{12}N_4P_2Pt$: C, 41.18; H, 4.27; N, 5.65. Found: C, 40.63; H, 4.26; N, 5.67. ^{1}H NMR (CD_3CN, δ): 0.95 (2H, m), 1.32 (2H, m), 1.55 (6H, m), 1.81 (2H, m), 2.50 (2H, dd, α-H, J_{H-H} = 18.0 and 10.0 Hz), 2.91 (2H, dd, α-H, J_{H-H} = 18.0 and 10.0 Hz), 3.07 (2H, d, α-H, J_{H-H} = 13.2 Hz), 3.40 (2H, d, α-H, J_{H-H} = 12.0 Hz), 3.73 (2H, dd, benzylic CH_2, J_{H-H} = 13.2 and 8.0 Hz), 3.86 (2H, dd, benzylic CH_2, J_{H-H} = 13.2 and 2.4 Hz), 7.07 (2H, d, J_{H-H} = 7.2 Hz), 7.16 (2H, dd, J_{H-H} = 9.2 and 7.6 Hz), 7.31 (2H, dd, J_{H-H} = 6.8 and 8.8 Hz), 7.59 (2H, dd, J_{H-H} = 6.4 and 8.4 Hz), 7.89 (2H, s, N−H), 7.89 (2H, d with Pt satellites, J_{H-Pt} = 60 Hz, J_{H-H} = 6.8 Hz), 8.22 (2H, d, J_{H-H} = 5.6 Hz), 8.29 (2H, dd, J_{H-H} = 8.0 and 9.6 Hz), 8.47 (2H, d, J_{H-H} = 8.0 Hz). MS-ESI (*m*/*z*): 846.27, $[Pt(pipNHC)_2(bpy)](PF_6)^+$.

[Pt(pipNHC)$_2$(dtfmbpy)](PF$_6$)$_2$. The product was isolated as a light-yellow solid by following the procedure for $[Pt(pipNHC)_2(bpy)](PF_6)_2$ and substituting 2,2′-bipyridine with dtfmbpy (29 mg, 0.1 mmol; *cis*-Pt(pipNC)$_2$, 54 mg, 0.1 mmol). Yield: 0.070 g, 62%. ^{1}H NMR (CD_3CN, δ): 1.15 (2H, m), 1.29 (2H, m), 1.57 (6H, m), 1.76 (2H, m), 2.39 (2H, dd, α-H, J_{H-H} = 13.6 and 6.0 Hz), 2.86 (2H, dd, α-H, J_{H-H} = 12.0 and 3.2 Hz), 3.02 (2H, dd, α-H, J_{H-H} = 12.0 and 3.0 Hz), 3.29 (2H, m, α-H), 3.87 (2H, dd, benzylic CH_2, J_{H-H} = 12.8 and 2.4 Hz), 4.06 (2H, dd, benzylic CH_2, J_{H-H} = 12.8 and 2.4 Hz), 7.16 (2H, dd, J_{H-H} = 8.0 and 3.2 Hz), 7.20 (2H, dd, J_{H-H} = 9.6 and 5.6 Hz), 7.36 (2H, dd, J_{H-H} = 8.0 and 2.4 Hz), 8.50 (2H, bs, N−H), 7.90 (2H, d with Pt satellites, J_{H-Pt} = 60 Hz, J_{H-H} = 13.2 Hz), 8.43 (2H, d, J_{H-H} = 9.6 Hz), 8.68 (2H, d, J_{H-H} = 5.6 Hz), 8.71 (2H, dd, J_{H-H} = 8.0 and 3.2 Hz). MS-ESI (*m*/*z*): 982.76, $[Pt(pipNHC)_2(dtfmbpy)](PF_6)^+$.

X-ray Crystallography.[12] Small orange-yellow blocks of Pt(pipNC)$_2$(phen) (**1**) were obtained by slow evaporation from a CH_2Cl_2-benzene-toluene solution. Yellow blocks of $[Pt(pipNHC)_2(phen)](PF_6)_2.2CH_3CN$ (**2**), $[Pt(pipNHC)_2(phen)](PF_6)_2$ (**3**), and $[Pt(pipNHC)_2(bpy)](PF_6)_2$ (**4**), as well as yellow plates of $[Pt(pipNHC)_2(dtfmbpy)](PF_6)_2.H_2O$ (**5**), were obtained by vapor diffusion of Et_2O vapors into acetonitrile or methylene chloride solutions of the respective salts. Colorless needles of *cis*-Pt(pipNC)$_2$ (**6**) were grown from *N*,*N*-dimethylformamide (DMF).

For X-ray examination and data collection, suitable crystals were mounted in a cryo-loop with paratone-N and transferred immediately to the goniostat bathed in a cold stream. Intensity data for *cis*-Pt(pipNC)$_2$ and $[Pt(pipNHC)_2(dtfmbpy)](PF_6)_2\cdot H_2O$ were collected using a Bruker APEX2 CCD detector, whereas data for Pt(pipNC)$_2$(phen) were collected using a Bruker Platinum200 CCD detector at Beamline 11.3.1 at the Advanced Light Source (Lawrence Berkeley National Laboratory) with synchrotron radiation tuned to λ = 0.775 Å. Intensity data for $[Pt(pipNHC)_2(phen)](PF_6)_2$, $[Pt(pipNHC)_2(phen)](PF_6)_2\cdot 2CH_3CN$, and $[Pt(pipNHC)_2(bpy)](PF_6)_2$ were collected using a Bruker SMART6000 CCD diffractometer with graphite-monochromated Cu Kα radiation, λ = 1.541 78 Å. Data were integrated using *SAINT* and corrected for decay and for Lorentz and polarization effects; absorption and beam corrections were applied based on a multiscan technique (*SADABS*).

Each structure was solved by a combination of direct methods (*SHELXTL* or *SIR*) and the difference Fourier technique and refined by full-matrix least squares on F^2 (*SHELXTL*). Non-H atoms were refined with anisotropic displacement parameters. $[Pt(pipNHC)_2(bpy)](PF_6)_2$ crystallizes with two independent molecules in the asymmetric unit (designated as A and B). The crystal used in the determination of Pt(pipNC)$_2$(phen) appeared to be a split crystal with a rotation of approximately 2° relating the two domains (CELL_NOW). The data were refined using a suitable twin law.

The N−H H atoms for both the solvated and nonsolvated forms of $[Pt(pipNHC)_2(phen)](PF_6)_2$ were located directly from the difference map, and the positions were refined; for $[Pt(pipNHC)_2(bpy)](PF_6)_2$ and $[Pt(pipNHC)_2(dtfmbpy)](PF_6)_2\cdot H_2O$, they were located directly and the positions were held fixed at that location. Likewise, the H atoms on the water solvent were located directly and the positions held fixed in subsequent refinements. All remaining H atoms in the structures were either located or calculated based on geometric criteria and treated with a riding model. The H-atom isotropic displacement parameters were defined as $1.2U_{eq}$ of the adjacent atom for the complex and $1.5U_{eq}$ of the adjacent atom for the solvate. Pt(pipNC)$_2$(phen) crystallizes with a disordered toluene molecule (~25% occupancy). A suitable disorder model was not forthcoming; thus, the solvate contribution was subtracted from the reflection data (*PLATON*). $[Pt(pipNHC)_2(phen)](PF_6)_2$ crystallizes with two molecules of CH_3CN in the lattice when grown from CH_3CN-Et_2O and as the nonsolvated form when grown from $CH_2Cl_2-Et_2O$, whereas $[Pt(pipNHC)_2(dtfmbpy)](PF_6)_2$ crystallizes as a hydrate from CH_3CN-Et_2O. For $[Pt(pipNHC)_2(dtfmbpy)](PF_6)_2\cdot H_2O$, several F atoms of the $-CF_3$ groups are disordered; however, a suitable multicomponent disorder model was not obtained. Disordered PF_6^- counterions were refined with multicomponent disorder models. Crystallographic data are summarized in Tables 1 and 2. Selected bond distances and angles are given in Table 3.

Results and Discussion

Synthesis. The synthesis of complexes with dangling nucleophilic groups at the axial sites of a square-planar metal center poses a significant challenge because of difficulties in forcing the metal to bond to one donor ligand over another. An efficient synthetic route to diarylplatinum(II) complexes with chelating diimine ligands and dangling amine groups is illustrated in Scheme 2. The products were characterized using ^{1}H NMR spectroscopy and mass spectrometry. Elemental analyses were in good agreement with the product formulations, with the exception of $[Pt(pipNHC)_2(dtfmbpy)](PF_6)_2$, which was consistently slightly high in C and H and low in N, possibly because of trace amounts of triphenylphosphine from the synthesis of dtfmbpy. *cis*-Pt(pipNC)$_2$ was prepared in ~60% yield following modification of the procedure for the synthesis of *cis*-Pt(2-Me$_2$NCH$_2$C$_6$H$_4$)$_2$.[13] The reaction yielded exclusively the cis isomer, as confirmed by the magnitude[14]

(12) (a) *APEX2 v1.0-27, 2.1-4, v2.0-2, SMART v5.631, and SAINT v6.45A, v7.06A, v7.34A*; Bruker AXS, Inc.: Madison, WI. (b) Sheldrick, G. M. *SADABS v2.10*; University of Göttingen: Göttingen, Germany; 2008. (c) Sheldrick, G. M. *CELL_NOW*, University of Göttingen: Göttingen, Germany, 2005. (d) Sheldrick, G. M. *SHELXTL v6.14*; Bruker AXS, Inc.: Madison, WI. (e) PLATON v210103: Spek, A. L. *Acta Crystallogr.* **1990**, *A46*, C34. (f) Brandenburg, K. *Diamond v3.2c*; Crystal Impact: Bonn, Germany. (g) SIR2004 v1.0: Burla, M. C.; Camalli, M.; Carrozzini, B.; Cascarano, G. L.; Giacovazzo, C.; Polidori, G.; Spagna, R. *J. Appl. Crystallogr.* **2003**, *36*, 1103.

(13) van der Ploeg, A. F. M. J.; van Koten, G.; Schmitz, J. E. J.; van der Linden, J. G. M. *Inorg. Chim. Acta* **1982**, *58*, 53–58.

(14) Longoni, G.; Fantucci, P.; Chini, P.; Canziani, F. *J. Organomet. Chem.* **1972**, *39*, 413–425.

Table 1. Crystal and Structure Refinement Data for **1**–**3**

	1	**2**	**3**
formula	$C_{36}H_{40}N_4Pt$	$[C_{36}H_{42}N_4Pt](PF_6)_2 \cdot 2CH_3CN$	$[C_{36}H_{42}N_4Pt](PF_6)_2$
fw, g/mol	723.81	1097.87	1015.77
cryst syst	monoclinic	triclinic	triclinic
space group	$P2_1/n$	$P\bar{1}$	$P\bar{1}$
a, Å	11.202(2)	11.3849(3)	10.5423(2)
b, Å	17.076(3)	12.3342(3)	12.2067(2)
c, Å	18.359(4)	17.2114(4)	15.9387(3)
α, deg	90	93.346(1)	86.019(1)
β, deg	103.796(6)	101.915(1)	71.343(1)
γ, deg	90	112.898(1)	72.672(1)
V, Å^3/Z	3410.6(12)/4	2152.52(9)/2	1871.95(6)/2
ρ_{calcd} (g/cm^3)	1.410	1.694	1.802
μ, mm^{-1}	5.132	7.601	8.664
T, K	173(2)	150(2)	150(2)
reflns collected	27 892	18 401	15 685
indep reflns, R_{int}	5772/0.0650	7421/0.0235	6415/0.0227
R1/wR2 [$I > 2\sigma(I)$][a]	0.0486/0.0979	0.0229/0.0566	0.0313/0.0786
R1/wR2 (all data)[a]	0.0575/0.1011	0.0236/0.0570	0.0342/0.0803

[a] $R1 = \sum||F_o| - |F_c||/\sum|F_o|$, $wR2 = [\sum w(F_o^2 - F_c^2)^2/\sum w(F_o^2)^2]^{1/2}$.

Table 2. Crystal and Structure Refinement Data for **4**–**6**

	4	**5**	**6**
formula	$[C_{34}H_{42}N_4Pt](PF_6)_2$	$[C_{36}H_{40}N_4F_6Pt](PF_6)_2 \cdot H_2O$	$C_{24}H_{32}N_2Pt$
fw, g/mol	991.75	1145.77	543.61
cryst syst	monoclinic	monoclinic	orthorhombic
space group	Cc	Cc	$Pbca$
a, Å	26.0414(5)	21.3160(10)	10.751(2)
b, Å	11.3056(2)	17.1154(10)	19.283(4)
c, Å	25.2438(5)	13.3214(6)	19.935(4)
α, deg	90	90	90
β, deg	93.313(1)	120.459(1)	90
γ, deg	90	90	90
V, Å^3/Z	7419.7(2)/8	4189.3(4)/4	4132.7(14)/8
ρ_{calcd} (g/cm^3)	1.776	1.817	1.747
μ, mm^{-1}	8.724	4.391	8.426
T, K	150(2)	200(2)	150(2)
reflns collected	30 383	23 246	39 678
indep reflns, R_{int}	12 271/0.0364	9155/0.0714	3778/0.1048
R1/wR2 [$I > 2\sigma(I)$][a]	0.0238/0.0589	0.0413/0.0954	0.0284/0.0661
R1/wR2 (all data)[a]	0.0241/0.0590	0.0460/0.0983	0.0438/0.0737

[a] $R1 = \sum||F_o| - |F_c||/\sum|F_o|$, $wR2 = [\sum w(F_o^2 - F_c^2)^2/\sum w(F_o^2)^2]^{1/2}$.

Table 3. Selected Distances and Angles for **1**–**5**

	1	**2**	**3**	**4A**[a]	**4B**[a]	**5**
Pt–C13	2.012(8)	2.024(3)	2.030(4)	2.035(4)	2.040(4)	2.024(5)
Pt–N1	2.110(6)	2.114(2)	2.123(3)	2.111(3)	2.117(3)	2.097(9)
Pt–N2	2.094(6)	2.120(2)	2.116(3)	2.108(3)	2.105(4)	2.097(5)
Pt–C25	2.017(7)	2.024(3)	2.016(4)	2.027(4)	2.028(4)	2.036(13)
Pt···N3	4.726(7)	4.634(2)	3.258(3)	3.187(3)	3.197(3)	3.290(5)
Pt···N4	4.668(7)	3.192(2)	3.214(3)	3.345(4)	3.327(3)	4.519(6)
Pt···H3		2.40(4)	2.33	2.32	2.37	2.51
Pt···H4		5.22(3)	2.34	2.47	2.49	5.17
N1–Pt–N2	79.7(2)	79.12(9)	79.19(13)	78.33(13)	77.99(13)	77.6(2)
N1–Pt–C13	93.5(2)	94.58(10)	96.80(14)	95.53(14)	96.27(14)	96.3(3)
C13–Pt–C25	93.1(3)	91.72(10)	89.57(15)	90.26(15)	89.25(15)	90.7(3)
N2–Pt–C25	94.0(2)	94.90(9)	94.42(14)	95.69(14)	96.46(14)	95.2(3)
N2–Pt–Cl3	171.9(3)	171.83(9)	174.14(13)	173.74(13)	174.26(13)	172.6(2)
N1–Pt–C25	172.7(3)	172.85(10)	173.61(13)	171.38(15)	173.81(14)	172.04(19)
N3–H3–Pt			155	148	141	153
N4–H4–Pt		150(3)	153	152	146	

[a] **4** crystallizes as two independent molecules (A and B) in the asymmetric unit.

of the $J(^{195}Pt-^{1}H)$ coupling constant and X-ray crystallography. The nearly colorless compound gives rise to intense yellow luminescence in the solid state and is very soluble in chloroform and methylene chloride but much less soluble in DMF and only sparingly soluble in acetonitrile.

Scheme 2. Synthetic Scheme[a]

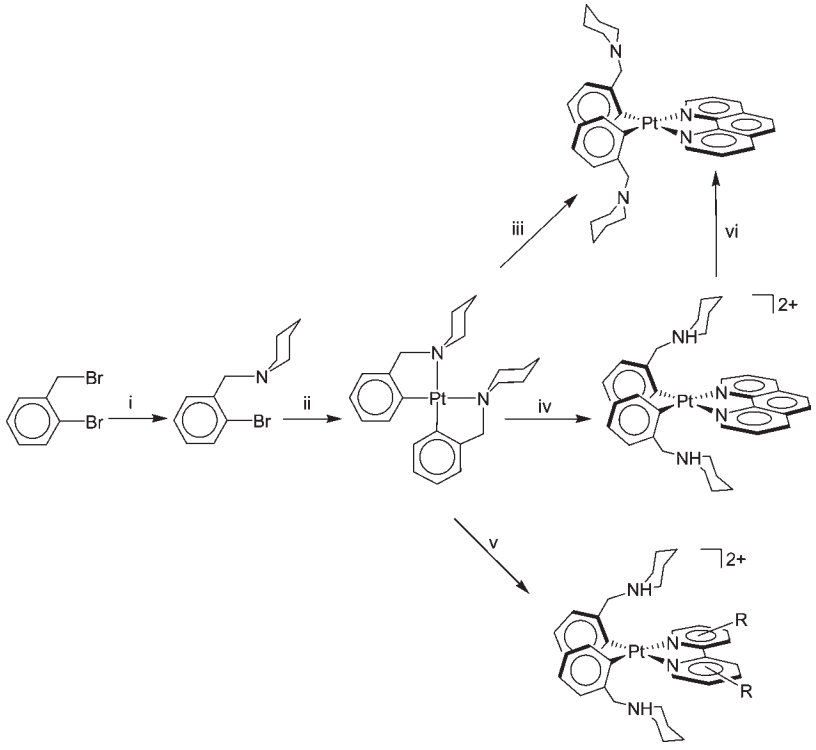

[a] Conditions: (i) piperidine/benzene, reflux; (ii) *n*-BuLi, $Pt(COD)Cl_2$/THF, −70 °C; (iii) 1,10-phenanthroline/CH_2Cl_2, reflux; (iv) TFA, 1,10-phenanthroline/CH_3CN, reflux; (v) (a) TFA, 2,2′-bipyridine/CH_3CN, reflux, (b) TFA, 5,5′-ditrifluoromethyl-2,2′-bipyridine/CH_3CN, reflux; (vi) TBAOH.

Refluxing *cis*-$Pt(pipNC)_2$ with phen in dichloromethane gives an apparent equilibrium mixture of $Pt(pipNC)_2$(phen) and starting materials. Because dissociation of the phen ligand is slow (vide infra), the $Pt(pipNC)_2$(phen) complex can be isolated from this mixture. The dissociation reactions of the bpy and dtfmbpy analogues are more rapid. For example, attempts to prepare the bpy adduct by the same procedure resulted in the expected change in solution color from colorless to yellow-orange, but efforts to isolate the product yielded only starting materials. On the other hand, hexafluorophosphate salts of the protonated adducts of each of the three diimine complexes, $Pt(pipNHC)_2(diimine)^{2+}$, were readily prepared in 60−70% yield from the reaction of the diimine ligand with an acidic solution of *cis*-$Pt(pipNC)_2$ (Scheme 2). Best results were obtained when *cis*-$Pt(pipNC)_2$ was completely dissolved in an acetonitrile solution with 2 equiv of trifluoroacetic acid prior to the addition of the diimine. The resulting protonated adducts are stable in an acetonitrile and methylene chloride solution and can be treated with 2 equiv of base to give transiently stable solutions of the deprotonated complexes.

Crystal Structures. The structures of *cis*-$Pt(pipNC)_2$ and $Pt(pipNC)_2$(phen), as well as salts of the protonated adducts, $Pt(pipNHC)_2(phen)^{2+}$, $Pt(pipNHC)_2(bpy)^{2+}$, and $Pt(pipNHC)_2(dtfmbpy)^{2+}$, were confirmed by X-ray crystallography (Figure 1). The pip_2NC^- ligands of $Pt(pipNC)_2$ adopt a cis configuration with 80.53(19)° (C1−Pt−N1) and 80.11(19)° (C13−Pt−N2) bite angles. To alleviate steric repulsion between the aryl and piperidyl groups, the complex is tetrahedrally distorted, resulting in a dihedral angle between the C1−Pt−N1 and C13−Pt−N2 planes of 13.1(2)° and nonzero ligand backbone torsion angles [C1−C6−C7−N1, 36.7(6)°; C13−C18−C19−N2, 34.8(6)°]. On the other hand, for the four compounds with diimine ligands, the coordination geometry is closer to square-planar. The $pipNC^-$ and pipNHC groups accommodate the chelating diimine ligand by rotation of the planar aryl groups out of the coordination plane defined by the Pt atom and the four nearest-neighbor atoms, resulting in dihedral angles of 86.8(2)−88.0(3)° for $Pt(pipNC)_2$(phen) and 55.0(1)−78.3(2)° for the three protonated adducts. The resulting Pt−N(diimine) distances [2.094(6)−2.123(3) Å] fall within the range observed for related complexes with aryl groups trans to monodentate pyridyl or bidentate diimine ligands [2.08(1)−2.201(2) Å].[15−25] These distances are substantially longer than those observed for monodentate pyridyl

(15) Jude, H.; Krause Bauer, J. A.; Connick, W. B. *Inorg. Chem.* **2004**, *43*, 725–733.
(16) Jude, H.; Krause Bauer, J. A.; Connick, W. B. *Inorg. Chem.* **2005**, *44*, 1211–1220.
(17) Kuehl, C. J.; Arif, A. M.; Stang, P. J. *Org. Lett.* **2000**, *2*, 3727–3729.
(18) Albinati, A.; Lianza, F.; Pregosin, P. S.; Mueller, B. *Inorg. Chem.* **1994**, *33*, 2522–2526.
(19) Chase, P. A.; Lutz, M.; Spek, A. L.; van Klink, G. P. M.; van Koten, G. *J. Mol. Catal. A: Chem.* **2006**, *254*, 2–19.
(20) Romeo, R.; Arena, G.; Scolaro, L. M.; Plutino, M. R.; Bruno, G.; Nicoló, F. *Inorg. Chem.* **1994**, *33*, 4029–4037.
(21) Plutino, M. R.; Scolaro, L. M.; Albinati, A.; Romeo, R. *J. Am. Chem. Soc.* **2004**, *126*, 6470–6484.
(22) Debaerdemaeker, T.; Hohenadel, R.; Brune, H.-A. *J. Organomet. Chem.* **1988**, *350*, 109–114.
(23) Casas, J. M.; Fornies, J.; Martin, A. *J. Chem. Soc., Dalton Trans.* **1997**, *9*, 1559–1563.
(24) Sun, Y.; Ross, N.; Zhao, S.-B.; Huszarik, K.; Jia, W.-L.; Wang, R.-Y.; Macartney, D.; Wang, S. *J. Am. Chem. Soc.* **2007**, *129*, 7510–7511.
(25) Ong, C. M.; Jennings, M. C.; Puddephatt, R. J. *Can. J. Chem.* **2003**, *81*, 1196–1205.

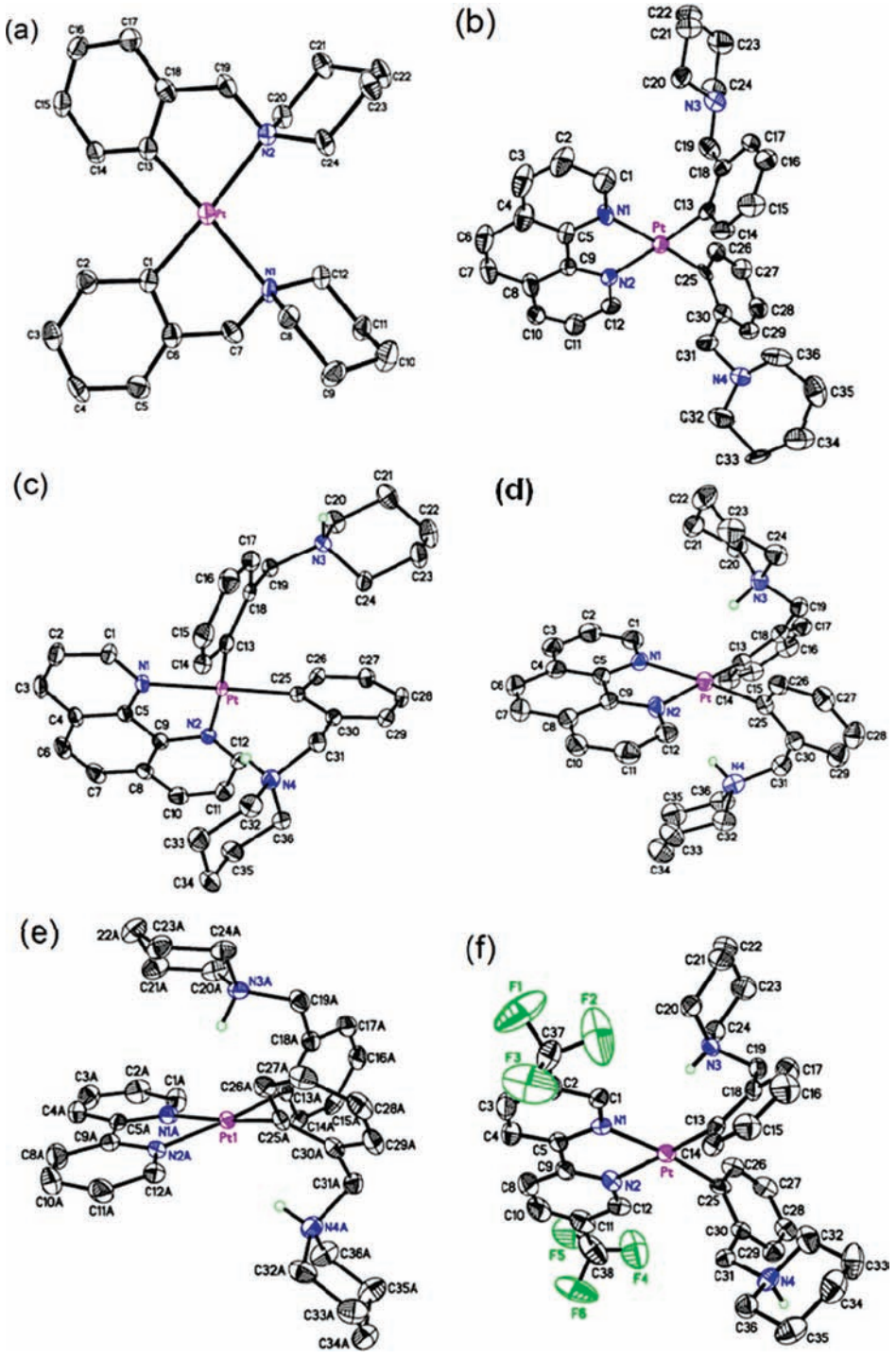

Figure 1. ORTEP diagram of (a) *cis*-Pt(pipNC)$_2$ and (b) Pt(pipNC)$_2$(phen) and cationic parts of (c) Pt(pipNHC)$_2$(phen)(PF$_6$)$_2$·2CH$_3$CN, (d) Pt(pipNHC)$_2$-(phen)(PF$_6$)$_2$, (e) Pt(pipNHC)$_2$(bpy)(PF$_6$)$_2$ (only one of the two independent molecules is shown), and (f) Pt(pipNHC)$_2$(dtfmbpy)(PF$_6$)$_2$·H$_2$O. H atoms [with the exception of those bonded to N(piperidyl)] are omitted for clarity. 50% probability thermal ellipsoids.

groups situated trans to ligands having a weaker trans influence[26] [e.g., Pt(phen)(en)$^{2+}$, 2.02(1) Å].[27] The Pt−C-(aryl) distances [2.012(8)−2.040(4) Å] are significantly longer than those found for *cis*-Pt(pipNC)$_2$ [Pt−C1, 1.980(5) Å; Pt−C(13), 1.985(5) Å] but within the range observed for compounds with pyridyl groups positioned trans to aryl ligands [1.910(3)−2.038(2) Å].[4,5,15,22,28]

For each diimine complex, the pipNC$^-$ and pipNHC groups adopt the more sterically favored head-to-tail conformation in which the piperidyl groups are directed toward opposite faces of the coordination plane. Interestingly, in crystals of Pt(pipNC)$_2$(phen), the piperidyl N atoms

(26) Connick, W. B.; Marsh, R. E.; Schaefer, W. P.; Gray, H. B. *Inorg. Chem.* **1997**, *36*, 913–922.

(27) Kato, M.; Takahashi, J. *Acta Crystallogr., Sect. C.: Cryst. Struct. Commun.* **1999**, *55*, 1809–1812.

(28) Jude, H.; Krause Bauer, J. A.; Connick, W. B. *Inorg. Chem.* **2002**, *41*, 2275–2281.

are directed away from the Pt atom [Pt···N4, 4.668(7) Å; Pt···N3, 4.726(7) Å], forming short intramolecular contacts with phenyl groups [N4···H29, 2.54 Å; N3···H17, 2.47 Å]. This arrangement is distinctly different from our observations for other platinum(II) complexes with dangling piperidyl groups, which typically show at least one short contact between a piperidyl N atom and the Pt^{II} center; for example, the crystal structure of [Pt(phtpy)(pip_2NCN)](BF_4) (phtpy = 4-phenyl-2,2′:6′,2″-terpyridine) reveals that each of the complexes in the asymmetric unit has a short Pt···N(piperidyl) contact [3.512(5) and 3.195(5) Å].[4] Each of those previously studied complexes is positively charged, and therefore the metal centers are expected to be more electrophilic than those for Pt(pip_2NC)(diimine). Interestingly, each of the four protonated complexes has at least one protonated piperidyl N atom directed toward the Pt atom, resulting in short NH···Pt distances (2.32−2.51 Å), which are significantly shorter than the sum of the van der Waals radii. In order to accommodate this interaction, the dihedral angles between the phenyl ring and the coordination plane fall in a relatively narrow range (55−65°). These results suggest that the Pt center has partial Brønsted base character, as is expected for proton-sponge-type behavior in which the protonated amine is stabilized by interaction with the nucleophilic metal center. Similar interactions have been noted by van Koten et al.[29,30] and others[18,23,31−33] for Pt^{II} centers with nearby protonated amine groups; in other cases, such interactions have not been observed.[34] In the present case, the geometric constraints of the pipNHC ligand result in bent NH···Pt (141−155°) angles and prevent a more linear arrangement, which would be optimal for a dipole−monopole interaction. Nevertheless, it is apparent that the geometries of the NH···Pt interactions are consistent with hydrogen bonding to the metal rather than three-center/two-electron agostic interactions.[18,32,35] Interestingly, in crystals containing Pt(pipNHC)$_2$(phen)$^{2+}$ and Pt(pipNHC)$_2$(dtfmbpy)$^{2+}$ with solvate molecules, the NH group of one of the piperidyl groups is directed toward the Pt center [Pt(pipNHC)$_2$(phen)$^{2+}$, NH···Pt, 2.40(4) Å; Pt(pipNHC)$_2$(dtfmbpy)$^{2+}$, NH···Pt, 2.51 Å], whereas the NH group of the other is directed toward a solvate molecule [Pt(pipNHC)$_2$(phen)$^{2+}$, NH···N(CH_3CN), 2.08(4) Å; Pt(pipNHC)$_2$(dtfmbpy)$^{2+}$, NH···N(H_2O), 1.90 Å; Figure S1 in the Supporting Information). For crystals containing Pt(pipNHC)$_2$(phen)$^{2+}$ and Pt(pipNHC)$_2$(bpy)$^{2+}$ without solvate, both piperidyl groups are directed toward the Pt center [Pt(pipNHC)$_2$(phen)$^{2+}$, NH···Pt, 2.33 and 2.34 Å; Pt(pipNHC)$_2$(bpy)$^{2+}$, NH···Pt, 2.32 and 2.47 Å for molecule A and 2.37 and 2.49 Å for molecule B). Thus, hydrogen bonding to solvate can effectively compete with the formation of a second intramolecular NH···Pt interaction.

^{1}H NMR Spectroscopy. The room-temperature ^{1}H NMR spectra of the protonated complexes show the expected pattern of resonances, and the spectra are concentration-independent over the investigated range (up to 0.01 M). Notably, in each case, one set of diimine resonances and four phenyl proton resonances are observed in the aromatic region. The benzylic proton resonances appear in an AB pattern near 3.8−3.9 ppm in CD_3CN solution for the phen and bpy complexes [between 4.1 and 3.8 ppm for Pt(pipNHC)$_2$(dtfmbpy)$^{2+}$], establishing that these protons are diastereotopic and that the coupling to the amine proton is weak. [In contrast, the benzylic proton resonances for *cis*-Pt(pipNC)$_2$ appear as a sharp singlet with ^{195}Pt satellites, indicating that relaxation of the tetrahedral distortion observed in the solid state is rapid on the NMR time scale.] For the protonated adducts, the α-piperidyl protons give rise to four distinct resonances with equal intensities from 2.5 to 3.2 ppm, and a similar pattern is observed upfield for the *β*-proton resonances. Taken together with the observations for the benzylic proton resonances, these data confirm that the combination of inversion about the piperidyl N and inversion of the piperidyl ring is slow on the NMR time scale, as was expected for a protonated piperidyl group. In addition, asynchronous rotation about the Pt−C bond must also be slow, as was expected from steric considerations.[36−39] Overall, the data are consistent with the presence of a single rotamer, which we hypothesize to be the head-to-tail isomer, as observed in the crystal structures and in keeping with the steric demands of the piperidyl groups. This configuration would allow for the possibility of two NH···Pt interactions.

The piperidyl NH protons give rise to a broadened resonance, which occurs near ∼8 ppm in CD_3CN for the phen and bpy complexes [8.5 ppm for Pt(pipNHC)$_2$(dtfmbpy)$^{2+}$]. It is shifted by ∼1.0 ppm downfield from that of Pt(pip_2NCNH_2)(tpy)$^{3+}$.[5] The Pt center in the latter complex is comparatively electron-poor, and there is no evidence of NH···Pt interactions. A downfield chemical shift of proton resonances from free ligand values is a signature of NH···Pt hydrogen bonding,[33,40] and our observations are consistent with this possibility. In DMF-d_7, the NH resonance shifts linearly upfield with temperature (9.10−8.83 ppm, 295−370 K; Figure S2 in the Supporting Information), whereas the other resonances are essentially unaffected; the water resonance undergoes a downfield shift of 0.61 ppm (from 3.49 to 2.88 ppm) over the same temperature range. However, we have not observed ^{195}Pt−^{1}H coupling in any solvent (CD_3CN, DMF-d_7, and CD_2Cl_2), and Casas et al. have cautioned that the mere observation of a downfield shift from the free ligand is not proof of a Pt−H bonding interaction.[23] For example, shielding due to paramagnetic anisotropy of the Pt^{II} ion

(29) Wehman-Ooyevaar, I. C. M.; Grove, D. M.; Kooijman, H.; van der Sluis, P.; Spek, A. L.; van Koten, G. *J. Am. Chem. Soc.* **1992**, *114*, 9916–9924.
(30) Albrecht, M.; Dani, P.; Lutz, M.; Spek, A. L.; van Koten, G. *J. Am. Chem. Soc.* **2000**, *122*, 11822–11833.
(31) Davies, M. S.; Fenton, R. R.; Huq, F.; Ling, E. C. H.; Hambley, T. W. *Aust. J. Chem.* **2000**, *53*, 451–456.
(32) Yao, W.; Eisenstein, O.; Crabtree, R. H. *Inorg. Chim. Acta* **1997**, *254*, 105–111.
(33) Brammer, L.; Charnock, J. M.; Goggin, P. L.; Goodfellow, R. J.; Orpen, A. G.; Koetzle, T. F. *J. Chem. Soc., Dalton Trans.* **1991**, 1789–1798.
(34) For example, see:Hinman, J. G.; Baar, C. R.; Jennings, M. C.; Puddephatt, R. J. *Organometallics* **2000**, *19*, 563–570.
(35) Brammer, L.; McCann, M. C.; Bullock, R. M.; McMullan, R. K.; Sherwood, P. *Organometallics* **1992**, *11*, 2339–2341.
(36) Rotondo, E.; Bruschetta, G.; Bruno, G.; Rotondo, A.; Di Pietro, M. L.; Cusumano, M. *Eur. J. Inorg. Chem.* **2003**, 2612–2618.
(37) Clement, O.; Macartney, D. H.; Buncel, E. *Inorg. Chim. Acta* **1997**, *264*, 117–124.
(38) Margiotta, N.; Fanizzi, F. P.; Kobe, J.; Natile, G. *Eur. J. Inorg. Chem.* **2001**, 1303–1310.
(39) Margiotta, N.; Papadia, P.; Fanizzi, F. P.; Natile, G. *Eur. J. Inorg. Chem.* **2003**, 1136–1144.
(40) Canty, A. J.; van Koten, G. *Acc. Chem. Res.* **1995**, *28*, 406–413.

also is expected to induce a significant downfield shift.[41] Therefore, the NMR evidence for the persistence of a NH···Pt interaction in solution for the protonated complexes can only be regarded as circumstantial.

In the ^{1}H NMR spectrum of Pt(pipNC)$_2$(phen) in CD_2Cl_2, one set of diimine resonances and four phenyl proton resonances are observed in the aromatic region. The benzylic protons give rise to *two* characteristic AB patterns centered at 4.09 ppm (J, 13.9 Hz; $\Delta\nu/J$, 3.7) and 3.93 ppm (J, 14.6 Hz; $\Delta\nu/J$, 7.1), respectively, in a 3:2 intensity ratio ($\Delta\nu$ is the chemical shift difference between the furthest upfield resonance and the furthest downfield resonance). These observations suggest that rotation of the phenyl group about the Pt−C bond remains slow on the NMR time scale. The two isomers present in unequal amounts are tentatively attributed to the head-to-tail and head-to-head conformers.

In CD_3CN, DMF-d_7, and CD_2Cl_2, the ^{1}H NMR spectrum of the deprotonated complex is time-dependent. For example, in DMF-d_7 and CD_2Cl_2, resonances associated with Pt(pipNC)$_2$(phen) gradually lose intensity, while resonances associated with *cis*-Pt(pipNC)$_2$ and the free phen ligand gain intensity, indicating the occurrence of ligand dissociation:

$$\text{Pt(pipNC)}_2\text{(phen)} \rightleftharpoons \textit{cis}\text{-Pt(pipNC)}_2 + \text{phen}$$

The reaction was monitored by a gradual decrease in the intensity of the coordinated phen ligand resonances relative to a TMS standard immediately following the addition of 2 equiv of TBAOH to a solution of Pt(pipNHC)$_2$(phen)$^{2+}$ (Figure S3 in the Supporting Information). The fraction of Pt(pipNC)$_2$(phen) remaining and the fraction of product formed as a function of time are approximately modeled by single-exponential functions. Under typical conditions ($\sim 10^{-2}$ M), the resulting decay constants were $10^{-5}-10^{-6}$ s^{-1}. After several days in CD_2Cl_2, the spectra ceased to change but showed the presence of both reactants and products, suggesting that an equilibrium had been established and, therefore, the back reaction of *cis*-Pt(pipNC)$_2$ and phen contributes to the observed dissociation kinetics. In a CD_3CN solution, the disappearance of Pt(pipNC)$_2$(phen) resonances is accompanied by precipitation. The ^{1}H NMR spectrum of the precipitate in a $CDCl_3$ solution confirms the presence of *cis*-Pt(pipNC)$_2$ (which is insoluble in CD_3CN) and free phen ligand, as well as a small fraction of an insoluble precipitate that remains unidentified. The disappearance of Pt(pipNC)$_2$(phen) resonances in a CD_3CN solution is considerably more rapid ($\sim 10^{-3}$ s^{-1}), as was expected for precipitation of products effectively driving the ligand dissociation reaction to completion. It is not presently known if other solvent effects, such as specific interactions between the solvent and complex, also play a significant role in the observed reactivity. ^{1}H NMR spectra of Pt(pipNC)$_2$(bpy) and Pt(pipNHC)$_2$(dtfmbpy) confirm that these complexes also undergo diimine ligand dissociation, albeit much more rapidly.

Electronic Spectroscopy. In order to assess the influence of the dangling piperidyl and piperidinium groups on the electronic structures of these complexes, electronic absorption spectra were recorded. *cis*-Pt(pipNC)$_2$ is a colorless solid, which dissolves in CH_2Cl_2 to give two intense bands, maximizing at 266 and 310 nm, respectively. The ligand precursor pipNCBr ($\varepsilon < 350$ M^{-1} cm^{-1}) and *N*-isopropylidenemethylamine ($\varepsilon < 100$ M^{-1} cm^{-1})[42,43] only absorb weakly at these wavelengths, indicating the involvement of the Pt center in the electronic transitions. The spectrum is very similar to that of *cis*-Pt(2-Me$_2$NCH$_2$C$_6$H$_4$)$_2$, and by analogy, the transitions are assigned as having significant metal-to-ligand charge-transfer (MLCT) character.[13]

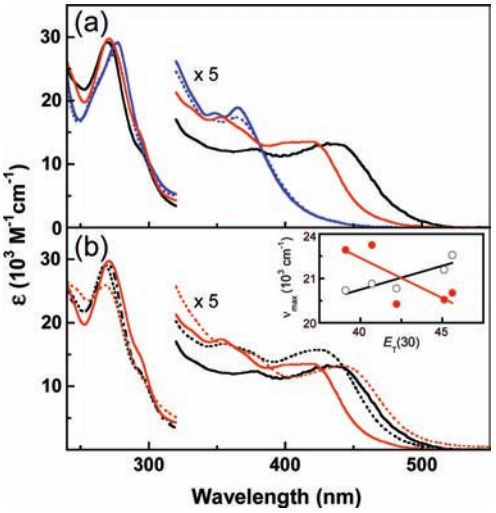

Figure 2. Electronic absorption spectra of Pt(phen)(Ph)$_2$ (CH_2Cl_2, —; CH_3CN, ---), Pt(pipNHC)$_2$(phen)$^{2+}$ (CH_2Cl_2, blue —; CH_3CN, blue ---), and Pt(pipNC)$_2$(phen) (CH_2Cl_2, red —; CH_3CN, red ---) in freshly prepared solutions. Longest wavelength absorption maximum (ν_{max}) vs E_T(30) of a series of solvents (left-to-right: chloroform, methylene chloride, acetone, DMSO, and acetonitrile) for Pt(phen)(Ph)$_2$ (○) and Pt(pipNC)$_2$(phen) (red ●); the lines show the linear best fit for the purpose of showing trends in the data.

For the diimine complexes, we have focused our attention on the phen derivatives and the Pt(phen)(phenyl)$_2$ model complex because of the greater stability of Pt(pipNC)$_2$(phen) compared to the other deprotonated adducts. The yellow protonated adducts, [Pt(pipNHC)$_2$(diimine)](PF$_6$)$_2$, dissolve in CH_2Cl_2, CH_3CN, and DMF to give yellow solutions, whereas Pt(pipNC)$_2$(phen) gives yellow-orange solutions. In keeping with the absorption spectra of related platinum(II) diimine compounds,[44−46] Pt(phen)(Ph)$_2$, Pt(pipNHC)$_2$(phen)$^{2+}$, and Pt(pipNC)$_2$(phen) each exhibit an intense ligand-centered transition, maximizing near 270−280 nm (20−30 000 M^{-1} cm^{-1}; Figure 2). Measurements in different solvents (methanol, acetonitrile, DMSO, acetone, methylene chloride, and chloroform) indicate that the absorption maxima are relatively insensitive to variations in Reichardt's E_T(30) solvent parameter,[47] with sensitivities comparable to those observed for ligand-centered transitions of Pt(bpy)Cl$_2$.[48]

(41) Buckingham, A. D.; Stephens, P. J. *J. Chem. Soc.* **1964**, 4583–4587.
(42) Brinton, R. K.; Chang, S. *Ber. Bunsenges. Phys. Chem.* **1968**, *72*, 217–221.
(43) Nelson, D. A.; Worman, J. J. *Tetrahedron Lett.* **1966**, 507–509.
(44) Fleeman, W. D.; Connick, W. B. *Comments Inorg. Chem.* **2002**, *23*, 205–230.
(45) Jin, V. X.; Ranford, J. D. *Inorg. Chim. Acta* **2000**, *304*, 38–44.
(46) Hissler, M.; Connick, W. B.; Geiger, D. K.; McGarrah, J. E.; Lipa, D.; Lachicotte, R. J.; Eisenberg, R. *Inorg. Chem.* **2000**, *39*, 447–457.
(47) Reichardt, C. *Chem. Rev.* **1994**, *94*, 2319–2358.
(48) Gidney, P. M.; Gillard, R. D.; Heaton, B. T. *J. Chem. Soc., Dalton Trans.* **1973**, 132–134.

Each of the complexes also exhibits several absorption features in the 350−380 nm range. The shoulders and maxima in this region are somewhat solvent-sensitive but do not track with polarity in an obvious pattern. The situation is likely complicated by overlapping bands with ligand-centered and MLCT character in this region.[45,49]

Platinum(II) phenanthroline complexes with phenyl donor ligands are reasonably expected to exhibit one or more MLCT transitions in the 400−500 nm region.[8] The stabilization of MLCT states under these circumstances is consistent with the strongly electron-donating ancillary ligands destabilizing the filled 5d(Pt) levels relative to the diimine π levels.[44,50] Therefore, it is not surprising that both the model complex [i.e., Pt(phen)$(Ph)_2$] and Pt-$(pipNC)_2$(phen) give rise to a long-wavelength absorption band in the 420−450 nm range (~2000 M^{-1} cm^{-1}; Figure 2). The longest-wavelength absorption profiles are qualitatively similar. Interestingly, in methylene chloride, the maximum for Pt$(pipNC)_2$(phen) is blue-shifted by 870 cm^{-1} from that of Pt(phen)$(Ph)_2$, whereas in acetonitrile, the maximum for Pt$(pipNC)_2$(phen) is red-shifted by 850 cm^{-1} from that of Pt(phen)$(Ph)_2$. In this respect, the situation is different from that found for Pt(tpy)$(pip_2NCN)^+$.[51] The electronic spectrum of the terpyridyl complex at wavelengths <500 nm is similar to that of the Pt(tpy)(2,6-dmph)$^+$ model complex. However, whereas the model complex is essentially nonabsorbing at >500 nm, Pt(tpy)$(pip_2NCN)^+$ shows a new absorption band, appearing as a weak shoulder near 550 nm (~300 M^{-1} cm^{-1}), which has been attributed to interaction of the dangling piperidyl group with the metal center. The absence of similar evidence of Pt···N-(piperidyl) interactions in Pt$(pipNC)_2$(phen) is consistent with the lower electrophilicity of the metal center of this complex compared to Pt(tpy)$(pip_2NCN)^+$. On the other hand, there are surprising differences in the solvent sensitivities of the longest-wavelength MLCT bands of Pt(phen)$(Ph)_2$ and Pt$(pipNC)_2$(phen), pointing to the subtle influence of the dangling piperidyl groups on the electronic structure. As expected,[8] the band for Pt(phen)-$(Ph)_2$ exhibits negative solvatochromism, shifting to longer wavelength with decreasing solvent polarity; the dependence on E_T is comparable to that noted for MLCT transitions of Pt(bpy)Cl_2.[48] Interestingly, although the maximum for Pt$(pipNC)_2$(phen) typically lies within 1000 cm^{-1} of that for Pt(phen)$(Ph)_2$ in most solvents, the band exhibits a distinctly *positive* solvatochromic behavior (inset, Figure 2). In other words, the solvent sensitivities of the long-wavelength band are approximately reversed for Pt-$(pipNC)_2$(phen) (CH_3CN, 441 nm; CH_2Cl_2, 421 nm) and Pt(phen)$(Ph)_2$ (CH_3CN, 425 nm; CH_2Cl_2, 437 nm). The reason for these differences is not certain, and the possibility that positive solvatochromism is a characteristic of apical Pt^{II}···N interactions is currently under investigation.

Protonation of the piperidyl groups has a dramatic effect on the longest-wavelength band, causing it to disappear entirely (or blue shift by >2500 cm^{-1}) or become obscured by other transitions at wavelengths <400 nm. This remarkable influence of the protonated piperidyl groups on the MLCT energies exceeds expectations for a through-bond inductive effect because the piperidinium N atoms are four and five covalent bonds removed from the metal center and diimine ligands, respectively. We attribute this behavior to axial NH···Pt interactions, which effectively reduce the electron density at the metal center and thereby destabilize MLCT states. Consistent with intramolecular interactions rather than intermolecular interactions, we note that, over the concentration range of these measurements (up to 0.2 mM), the spectra obey Beer's law. Although the proton-acceptor properties of Pt^{II} centers are well documented,[18,23,29−33] little attention has been given to the influence of these interactions on the electronic structures of the complexes. The gradual addition of 1 equiv of base to a solution of Pt$(pipNHC)_2(phen)^{2+}$ in CH_2Cl_2 causes the longest-wavelength tail of the absorption spectrum to broaden and shift slightly (~800 cm^{-1}) to the red (Figure 3a). The gradual addition of a second 1 equiv shifts the longest-wavelength absorption maximum by an additional 2800 cm^{-1} to the red (Figure 3b). Both titration steps exhibit sharp isosbestic points characteristic of an A → B → C process. These observations are consistent with significantly different pK_a values for the mono- and diprotonated adducts, as would be expected if the protons interact with the metal center on opposite faces of the coordination plane.

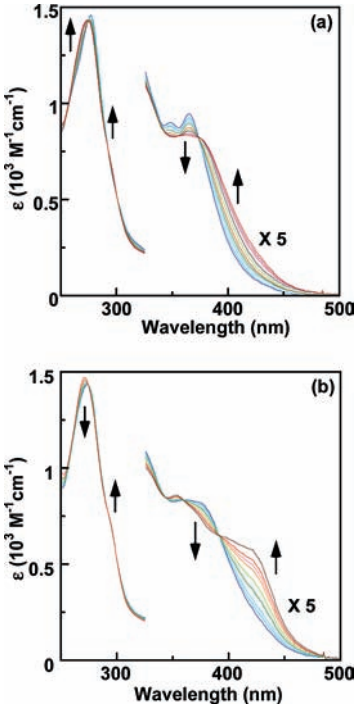

Figure 3. UV−visible absorption spectra recorded during the addition of 100 μM TBAOH to a 50 μM solution of [Pt$(pipNHC)_2$(phen)]$(PF_6)_2$ in CH_2Cl_2. The addition of (a) 1 equiv and (b) a second 1 equiv in 0.1 M increments.

Electrochemistry. To assess the influence of the dangling piperidinium and piperidyl groups on the redox properties of Pt$(pipNHC)_2(phen)^{2+}$ and Pt$(pipNC)_2$-(phen), respectively, cyclic voltammograms (CVs) were recorded in a 0.1 M $TBAPF_6$−methylene chloride solution (Figure 4). The CV of Pt$(pipNHC)_2(phen)^{2+}$ (0.75 V/s, gold working electrode) shows no oxidation at potentials

(49) Miskowski, V. M.; Houlding, V. H. *Inorg. Chem.* **1989**, *28*, 1529–1533.
(50) Connick, W. B.; Miskowski, V. M.; Houlding, V. H.; Gray, H. B. *Inorg. Chem.* **2000**, *39*, 2585–2592.
(51) The absorption spectrum of the latter complex in CH_2Cl_2 shows a distinct shoulder near 550 nm which is absent from the spectrum of the Pt(tpy)$(Ph)^+$ model compound.

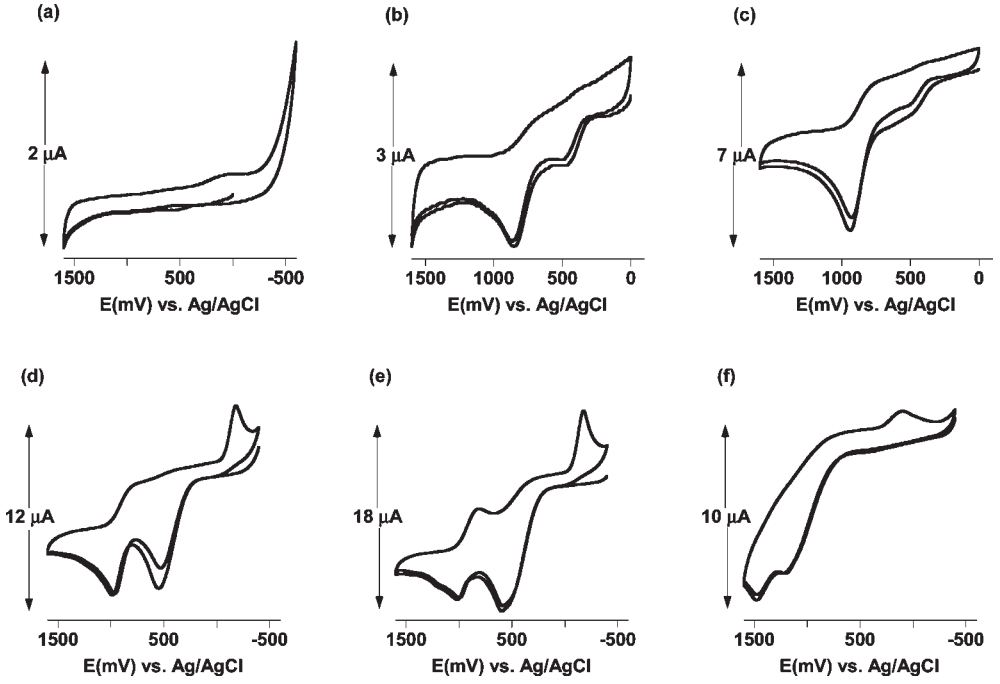

Figure 4. CVs of 1.0 mM $[Pt(pipNHC)_2(phen)](PF_6)_2$ (0.1 M $TBAPF_6$ in CH_2Cl_2) upon the addition of TBAOH at a sweep rate of 0.100 V/s (gold working electrode): (a) no added base; (b) 0.5 mM TBAOH; (c) 1.0 mM TBAOH; (d) 1.5 mM TBAOH; (e) 2.0 mM TBAOH; (f) 2.5 mM TBAOH.

< 1.5 V vs Ag/AgCl and two broad irreversible reduction waves at -0.6 and -0.75 V, respectively. The addition of 0.5 mol equiv of TBAOH resulted in the appearance of an irreversible wave characterized by an anodic peak (E_{pa}) maximizing near 0.8 V and a very weak feature near 0.45 V. The addition of 1 equiv of base caused a significant increase in the current near 0.8 V with little change at 0.45 V. On the other hand, the further addition of base (up to 2 equiv in total) caused a significant increase in the current associated with the 0.45 V feature *at the expense* of the current associated with the process at higher potential. The 0.45 V wave exhibited a slight splitting, suggesting two closely overlapping processes. The appearance of the 0.45 V wave was accompanied by a back-reduction process near -0.3 V. The latter reduction was only observed with sweeping initially in the anodic direction to a reversal potential $\gtrsim 0.45$ V, indicating that the electroactive species at -0.3 V ultimately originates from the oxidation process at 0.45 V. Even at scan rates up to 5 V/s, no reduction was observed at more positive potentials (i.e., > -0.3 V), suggesting that the electrochemical product generated at 0.45 V reacts rapidly to produce a chemical product (i.e., an EC mechanism). The overall chemical reversibility, as reported by the relative peak currents of the anodic 0.45 V wave and the cathodic -0.3 V wave, increases with an increase in the concentration of the base. The ratio of the peak currents also is scan-rate-dependent. At low scan rates (0.025 V/s), there was virtually no current associated with the back-reduction at 0.3 V, indicating that the 0.45 V electrochemical product is somewhat unstable. The addition of more than 2.5 equiv of base resulted in decomposition, which was demonstrated by the disappearance of the 0.45 and -0.3 V processes and a significant broadening of resonances in the ^1H NMR spectrum. The electrochemistry is qualitatively similar in DMF with similar values of E_{pa} (0.5 V) and E_{pc} (-0.2 V). The instability of $Pt(pipNC)_2(phen)$ in acetonitrile prevented an exhaustive study (E_{pa}, 0.35 V; E_{pc}, -0.2 V). The electrochemistry also is electrode-dependent. Notably, the return wave near -0.3 V is absent when using a platinum working electrode.

Because the observed electrochemical processes are irreversible, the peak potentials represent limiting values of the thermodynamic potentials. Therefore, the accumulated electrochemical data, in conjunction with the UV−visible titration results, establish that the monoprotonated adduct is oxidized at ≤ 0.8 V, whereas Pt(pipNC)(phen) is oxidized at ≤ 0.45 V vs Ag/AgCl. The irreversible oxidation of $Pt(pipNC)(pipNHC)(phen)^+$ near 0.8 V is reasonably attributed to either a pipNC-centered or metal-centered oxidation. For example, we note that the free ligand precursor, pipNCBr, exhibits an adsorption process at almost identical potentials (E_{pa}, 0.82 V, 100 mV/s). On the other hand, an argument for metal-centered oxidation could be made based on the observation that, because of the steric constraints of the mesityl ligands, $Pt(phen)(mesityl)_2$ exhibits a nearly reversible $Pt^{III/II}$ couple at $\sim$0.80 V vs Ag/AgCl (0.45 V vs Fc^+/Fc; 0.1 V/s; 0.1 M $TBAPF_6$ in THF).[8] Although the CVs of *cis*-$Pt(pipNC)_2$ (E_{pa}, 0.97 V) and $Pt(phen)(Ph)_2$ (E_{pa}, 1.17 V) show irreversible processes at slightly more positive potentials, the availability of a dangling piperidyl group at the axial site of $Pt(pipNC)(pipNHC)(phen)^+$ can be reasonably expected to decrease the $Pt^{III/II}$ redox potential.[3−5]

The oxidation of $Pt(pipNC)_2(phen)$ occurs at significantly more negative potentials than the oxidation of pipNCBr, $Pt(phen)(Ph)_2$, or $Pt(phen)(mesityl)_2$. Therefore, the wave at 0.45 V is tentatively attributed to oxidation of the metal center, which because of the instability of platinum(III) is expected to directly (or following chemical steps) yield platinum(IV) products. Consistent with this assignment, we note that the cathodic shift with respect to the $Pt^{III/II}$ couple of $Pt(phen)(mesityl)_2$ (0.80 V) is

in accordance with stabilization of the electrochemical products by interaction of the dangling piperidyl groups with the oxidized metal center. Attempts to assess electron stoichiometry by bulk electrolysis or spectroelectrochemistry were hampered by the instability of the electrochemical products. Nevertheless, accompanying UV−visible absorption measurements show a pronounced decrease in absorbance at wavelengths >325 nm. This behavior is qualitatively consistent with a metal-centered oxidation because bands with MLCT character are expected to blue-shift or to disappear altogether. The cathodic process near −0.3 V is tentatively assigned to the reduction of a platinum(III) or platinum(IV) product whose identity is not yet certain.

Although the chemical irreversibility of the oxidation process near 0.45 V prevents assessment of the electrochemical reversibility or extraction of precise thermodynamic information, it is noteworthy that the peak potential of the anodic process shows a characteristic dependence on the sweep rate, with E_{pa} undergoing a substantial anodic shift with an increase in the scan rate.[4,5,52,53] For example, E_{pa} increases from 0.42 to 0.77 V as the scan rate is varied from 0.05 to 4.0 V/s. Over the same scan rate range, E_{pc} of the cathodic process near −0.3 V decreases by only 0.06 mV (Figure S6 in the Supporting Information). In the case of the $Pt^{IV/II}$ couple of $Pt(tpy)(pip_2NCN)^+$, this pattern of behavior has been attributed to the formation of a preorganized structure, such as a five- or six-coordinate complex, prior to or during anodic electron transfer.[4,5] The conversion of six-coordinate platinum(IV) to four-coordinate platinum(II) and axial bond cleavage during the reverse (cathodic) process are likely to require less preorganization, making E_{pc} less sensitive to the scan rate. The anodic peak potential suggests that the formal $Pt^{IV/II}$ couple occurs at ≤0.45 V. To better gauge where this couple may reasonably lie, we have noted that investigations of six-coordinate ruthenium complexes show that substitution of a pyridyl group for a phenyl group [e.g., $Ru(bpy)_3^{3+/2+}$, 1.29 V; $Ru(bpy)_2$(2-phenylpyridine)$^{2+/+}$, 0.66 V vs SCE;[54] $Ru(tpy)_2^{3+/2+}$, 1.27 V; Ru(tpy)(6-phenyl-2,2′-bipyridine)$^{2+/+}$, 0.43 V vs SSCE][55,56] causes a 0.6−0.8 V cathodic shift in the $Ru^{III/II}$ redox couple. Therefore, by comparison to $Pt(tpy)(pip_2NCN)^+$ (0.4 V vs Ag/AgCl; 0.1 M $TBAPF_6$ in CH_3CN), and as expected for the increased σ/π-donor properties of phenyl versus a pyridyl group, the $Pt^{IV/II}$ couple of $Pt(pipNC)_2$(phen) is reasonably predicted to occur in the vicinity of −0.4 V for the analogous reaction. Thus, the appearance of E_{pa} for $Pt(pipNC)_2$(phen) near 0.45 V is suggestive of substantially decreased electrochemical reversibility in this system or even an entirely different mechanism. In this regard, it has occurred to us that the reduced electrophilicity of the Pt center of $Pt(pipNC)_2$(phen) compared to $Pt(tpy)(pip_2NCN)^+$ is likely to reduce the tendency to form the preorganized structure necessary to initiate metal-centered oxidation at relatively negative potentials.

Conclusions

An effective synthetic route to diarylplatinum(II) diimine complexes with two dangling piperidyl groups involves preparation of the diprotonated piperidinium adducts, $Pt(pipNHC)_2$(diimine)$^{2+}$. Deprotonation yields $Pt(pipNC)_2$(diimine) products. Crystallographic and spectroscopic data for the protonated complexes are consistent with NH···Pt interactions involving the piperidinium groups, suggesting that the metal center behaves as a Brønsted base. The geometries of the NH···Pt interactions in the solid state are consistent with hydrogen bonding to the metal rather than three-center/two-electron agostic interactions. NH···Pt interactions have a significant impact on the electronic structures of these complexes, strongly destabilizing MLCT states and inducing a substantial anodic shift in metal-centered redox processes. By contrast, N···Pt interactions in the deprotonated adducts, $Pt(pipNC)_2$(diimine), must be weak relative to outer-sphere two-electron reagents, such as $Pt(pip_2NCN)(tpy)^+$. Despite the low electrophilicity of the metal center, the deprotonated complexes undergo diimine ligand dissociation to give *cis*-$Pt(pipNC)_2$. It may be inferred that these reactions are initiated by coordination of a dangling piperdidyl group at the axial site of the square-planar complex.[57] In the case of $Pt(pipNC)_2$(phen), the presence of piperidyl groups also stabilizes higher oxidation states, in accordance with the notion that the amine groups are available to bind at the axial sites of the oxidized metal center. Nevertheless, the chemical and electrochemical reversibility is substantially lower than that of $Pt(pip_2NCNH_2)(tpy)^+$. We believe that a contributing factor is the lower electrophilicity of the metal center in $Pt(pipNC)_2$(phen), which is anticipated to decrease the tendency of the dangling piperidyl groups to interact at the open coordination sites compared to the tpy adduct. These interactions are expected to preorganize the complex for electron transfer, thereby increasing the rate of heterogeneous electron transfer. In addition, it would appear that the ligand denticity and conformational flexibility of $Pt(pipNC)_2$(phen) favor chemical steps following electron transfer that are comparatively slow in the case of a reagent with two potentially meridional-coordinating ligands (e.g., $Pt(pip_2NCN)(tpy)^+$).

Acknowledgment. Funding for the SMART6000 CCD diffractometer was through NSF-MRI Grant CHE-0215950. W.B.C. thanks the National Science Foundation (Grant CHE-0134975) for their generous support and the Arnold and Mabel Beckman Foundation for a Young Investigator Award. S.C. thanks the University of Cincinnati University Research Council for a summer fellowship, and the University of Cincinnati Industrial Affiliates Program for their generous support. We also thank Dr. Hershel Jude and Bonnie M. Young for helpful discussions. Synchrotron data were collected through the SCrALS (Service Crystallography at Advanced Light Source) project at Beamline 11.3.1 at the Advanced Light Source (ALS), Lawrence Berkeley National Laboratory. The ALS is supported by the U.S. Department of Energy, Office of Energy Sciences, under Contract DE-AC02-05CH11231.

Supporting Information Available: Figures S1−S6, Table S1, and crystallographic data in CIF format for all compounds. This material is available free of charge via the Internet at http://pubs.acs.org.

(52) Fernandes, J. B.; Zhang, L. Q.; Schultz, F. A. *J. Electroanal. Chem.* **1991**, *297*, 145–161.
(53) Uhrhammer, D.; Schultz, F. A. *Inorg. Chem.* **2002**, *43*, 7389–7395.
(54) Reveco, P.; Cherry, W. R.; Medley, J.; Garber, A.; Gale, R. J.; Selbin, J. *Inorg. Chem.* **1986**, *25*, 1842–1845.
(55) Constable, E. C.; Hannon, M. J. *Inorg. Chim. Acta* **1993**, *211*, 101–110.
(56) Morris, D. E.; Hanck, K. W.; DeArmond, K. *J. Electroanal. Chem.* **1983**, *149*, 115–130.
(57) Langford, C. H.; Gray, H. B. *Ligand Substitution Processes*; W. A. Benjamin, Inc.: Reading, MA, 1966.